

"An innovative bio-engineering retaining structure for supporting unstable soil"

*Original*

"An innovative bio-engineering retaining structure for supporting unstable soil" / Bella, Gianluca; Barbero, Monica; Barpi, Fabrizio; BORRI BRUNETTO, Mauro; Peila, Daniele. - In: JOURNAL OF ROCK MECHANICS AND GEOTECHNICAL ENGINEERING. - ISSN 1674-7755. - ELETTRONICO. - 9:(2017), pp. 247-259. [10.1016/j.jrmge.2016.12.002]

*Availability:*

This version is available at: 11583/2665865 since: 2021-04-02T10:45:00Z

*Publisher:*

ELSEVIER

*Published*

DOI:10.1016/j.jrmge.2016.12.002

*Terms of use:*

This article is made available under terms and conditions as specified in the corresponding bibliographic description in the repository

*Publisher copyright*

(Article begins on next page)



Contents lists available at ScienceDirect

# Journal of Rock Mechanics and Geotechnical Engineering

journal homepage: [www.rockgeotech.org](http://www.rockgeotech.org)

## Full Length Article

# An innovative bio-engineering retaining structure for supporting unstable soil



Gianluca Bella<sup>a,\*</sup>, Monica Barbero<sup>a</sup>, Fabrizio Barpi<sup>a</sup>, Mauro Borri-Brunetto<sup>a</sup>,  
Daniele Peila<sup>b</sup>

<sup>a</sup> DISEG, Politecnico di Torino, Corso Duca degli Abruzzi 24, Torino, 10129, Italy

<sup>b</sup> DIATI, Politecnico di Torino, Corso Duca degli Abruzzi 24, Torino, 10129, Italy

## ARTICLE INFO

### Article history:

Received 28 June 2016

Received in revised form

8 December 2016

Accepted 15 December 2016

Available online 21 February 2017

### Keywords:

Bio-engineering

Test site

Landslide

Live cribwall

Unstable soil

## ABSTRACT

The paper presents a new prefabricated bio-engineering structure for the support of unstable soil. This prefabricated structure is made of a steel frame which is completely filled with soil and a face made of tree trunks among which scions or autochthonous bushes are planted. Due to the difficulties in interpreting the complex interaction between soil and structure during the installation and lifetime, an in situ test was carried out in order to evaluate the state of stress in the steel frame and to understand the global behavior of the structure under service loads. On the basis of the obtained results, a procedure for checking the structure safety was proposed and discussed. An easy design method was developed during the research. Moreover, the use of this type of prefabricated structure shows several advantages, such as good performances in terms of stabilizing effects, and easy assembly and transport.

© 2017 Institute of Rock and Soil Mechanics, Chinese Academy of Sciences. Production and hosting by Elsevier B.V. This is an open access article under the CC BY-NC-ND license (<http://creativecommons.org/licenses/by-nc-nd/4.0/>).

## 1. Introduction

Bio-engineering measures for shallow landslide stabilization, erosion prevention and/or control are widely used in engineering practice (Greenway, 1987; Victor and Bary, 1997; Morgan and Rickson, 2004; Norris et al., 2008). To achieve the desired engineering goals, live plants and natural elements such as tree trunks or stones can be used (Gray and Sotir, 1996; Campbell et al., 2006). Live cribwalls, vegetated rock gabions, vegetated rock, walls and joint plantings are common soil bio-engineering techniques that use “porous structures”, through which vegetative cuttings are inserted and established. These structural elements provide resistance to sliding, erosion and washout immediately after the installation. As soon as vegetation becomes established, plant roots invade and permeate the external face of the slope and the tree trunks, binding them together into a unified, coherent mass. Over time, the structural elements decrease in importance as the vegetation increases in strength and functionality (USDA and NRCS, 1992).

Over a century, the most widely used structure in bio-engineering has been the double cribwall or some variation on this basic scheme, such as the cribwalls named Vesuvio, Roma or Latina (Greenway, 1987; Cornellini, 2001; Cornellini and Sauli, 2005, 2012) whose composition is complex and subsequently the realization will be more expensive (Fig. 1). The realization of cribwalls, also called retaining structures or mixed wood-rocks structures (Fig. 2a and b), makes use of tree trunks and nowadays they are designed and used as gravity walls to resist shallow displacements, namely for the reshaping of unstable slopes or at the toe of embankments.

In some cases, a larger mechanical strength is needed, so the use of a retaining structure not completely biodegradable would be more suitable (Carbonari and Mezzanotte, 2000; De Antonis and Molinari, 2003; Stokes et al., 2004, 2007, 2010, 2014). Following this observation, a new hybrid prototype has been developed and presented in this paper. It is made of a prefabricated steel frame lying on the ground, and a wooden frame where vegetation is established (Gray and Sotir, 1996). This prototype, called “palificata viva loricata Terrasafe” (pLT), has been subjected to an extensive set of full-scale in situ tests to verify the states of strain and stress in the steel frame and in the wooden elements. Moreover, the complex interaction between soil and structure has been investigated. The installation of the pLT is quick and easy due to the usage of prefabricated elements consisting of tree trunks and metal profiles

\* Corresponding author.

E-mail address: [gianluca.bella@polito.it](mailto:gianluca.bella@polito.it) (G. Bella).

Peer review under responsibility of Institute of Rock and Soil Mechanics, Chinese Academy of Sciences.

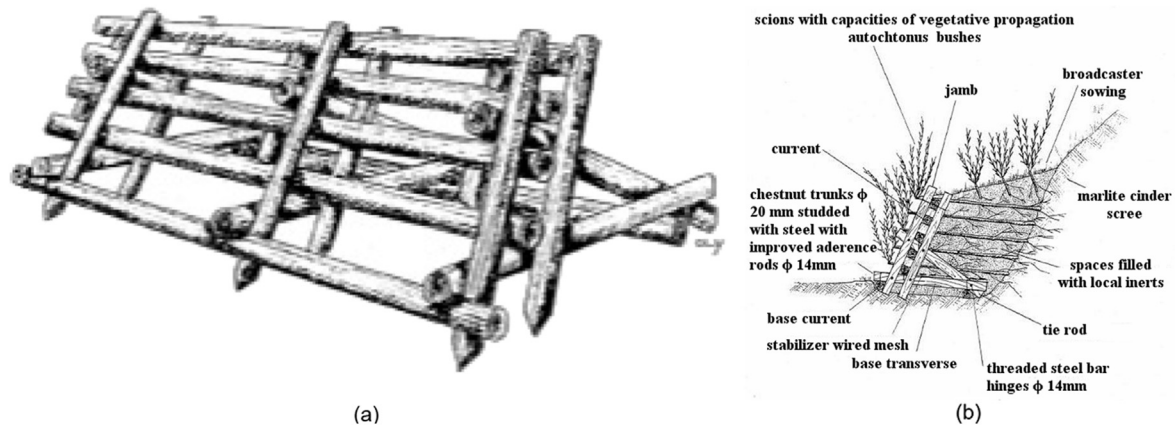


Fig. 1. Roma double cribwall (a) perspective, and (b) cross-section (modified from [Provincia di Terni, 2003](#)).

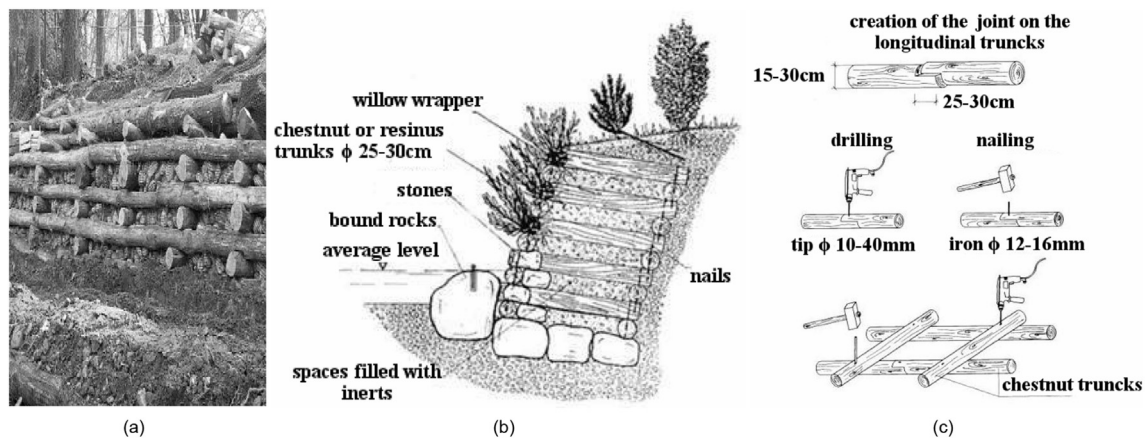


Fig. 2. (a) Double cribwall, and (b) its scheme and (c) construction phases (modified from [Provincia di Terni, 2003](#)).

that are light and easy to transport. The trunks are previously cut following the planned measure and do not need fastening with nails and bolts, thus eliminating the drilling. Furthermore, the pIT is a durable structure due to the non-biodegradability of its metal elements. Finally, the pIT is easily maintainable and environmental sustainable by replacing the trunks of the front face.

The experimental activities consist in the realization of a test site, in which some parts of the pIT were assembled and properly instrumented in order to verify its behavior under applied load. After the experimental study, a structural design method has been proposed, based on the principles of the European regulation [EN 1997-1 \(2004\)](#) for assessment of structural safety which is described in the paper. The prototype was verified from the structural and geotechnical point of view, letting to say the proposed design method can be considered reliable. For these reasons, the pIT is currently used as sustainable solution to some shallow landslides stabilization (i.e. Roatto and Fuscaldo, Italy). The strains measured by transducers were significantly lower than those calculated within the ultimate limit state theory, allowing to understand that the uniform overload applied on the pIT during the experimental campaign was not equal to that required for the mobilization of the active thrust.

## 2. Description of the structure and test site

The single element of the pIT, considered as a set of steel support and tree trunks ([Figs. 3 and 4](#)), is 3 m wide and 1.8 m high. The wooden frame is inclined by 60° with respect to the

horizontal line. The resistant structure consists in a frame made of steel sections, welded or bolted together, ending with a stem connected to an anchor plate, a rope or a bar anchor cemented into the ground.

A transverse horizontal beam is attached to the stem, and two uprights are welded to the cross and sustain the front trunks that are restrained by a chain to prevent large outward movements. The trunks create a grating that provides support for the filling soil and, not being continuous and closed, allows the planting of cuttings and facilitates drainage. Geometric and mechanical characteristics of the structural elements are as follows ([Fig. 3](#)):

- (1) Stem: hollow steel section UNI EN 10210 50 mm × 50 mm × 3 mm S235JRH;
- (2) Uprights and transversal beam: hollow steel section UNI EN 10210 70 mm × 70 mm × 3 mm S235JRH;
- (3) Foundation: steel plate 750 mm × 750 mm × 5 mm;
- (4) Six wooden trunks with 160–200 mm diameter and 3 m length.

Geometric sizes of the steel structure (1 kN weight) can be summarized as follow:

- (1)  $l = 0.75$  m (side of the foundation plate);
- (2)  $h = 1.8$  m (height of the structure);
- (3)  $d = 3$  m (depth of a standard module of structure);
- (4)  $\alpha = \beta = 30^\circ$  (angle between the front grid and the vertical line);

- (5)  $b = h \tan \alpha = 1.04 \text{ m}$ ;
- (6)  $c = 0.785 \text{ m}$  (half length of the horizontal beam).

In testing phases, chestnut debarked trunks (total weight equal to 3 kN) were used. In practice, larch trunks or other species can be adopted, depending on the characteristics of the installation site and design specifications. The debarking of trunks is strongly recommended because it is critical for the longevity of the wood by preventing the establishment of many animals, fungi and other vectors that speed its decay.

The assembly phases of the structure are summarized below:

- (1) Preparation of the support surface of the structure, which should be made flat, possibly by digging.
- (2) Positioning of anchorage plate or injected anchor, following the design prescriptions.
- (3) Assembly of the structure in a suitable place.
- (4) Installation of the metal structure and its connection to the anchor.
- (5) Positioning of the trunks.
- (6) Filling with soil (Fig. 5a). This operation can be carried out by acting either from upslope or from downslope. The filling soil must be compacted.
- (7) Alignments can be made on multiple lines after finishing the filling phase of the bottom row (Figs. 5b and 6).

Operational variations in this sequence may be caused by local aspects of the yards, because this modular structure can be easily transported in many parts and then assembled on site.

In order to evaluate the stresses induced in the structure by applying the loads during installation phases and lifetime, a test site in real scale has been created and some elements of pIT were installed. The pIT was instrumented to detect the following items:

- (1) The longitudinal strain in some sections of the steel frame using strain gage transducers (Fig. 7a);
- (2) The displacement and the stress of the anchor plate using linear variable differential transformer (LVDT) and load cells, respectively (Figs. 8 and 9a);
- (3) The global displacement of some points of the structure by using four topographic targets connected to the steel frame and installed on the front part of the pIT. Their positions were monitored during the test using a Leica total topographical station placed at a distance of about 15 m in front of the pIT (Fig. 9b).

The test site is a sand pit in Castello di Annone (Asti, Italy), whose soil has been used for the filling of the experimental prototype. The sand was classified in terms of grain size distribution (Fig. 10) and characterized in terms of shear strength (Table 1) by performing direct shearing tests at different density values. A friction angle, between those obtained at peak and those at critical state, was chosen equal to  $\varphi' = 40^\circ$ . The heterogeneity of the face of the structure, made of steel and tree trunks, leads to an assumption that the friction angle  $\delta$  between the filling soil and the face is equal to that of the filling soil ( $\varphi' = \delta$ ). Considering that the specific weight of the soil  $\gamma$  is equal to  $15 \text{ kN/m}^3$ , the friction angle  $\delta_a$  between the foundation plate and the filling soil is then assumed

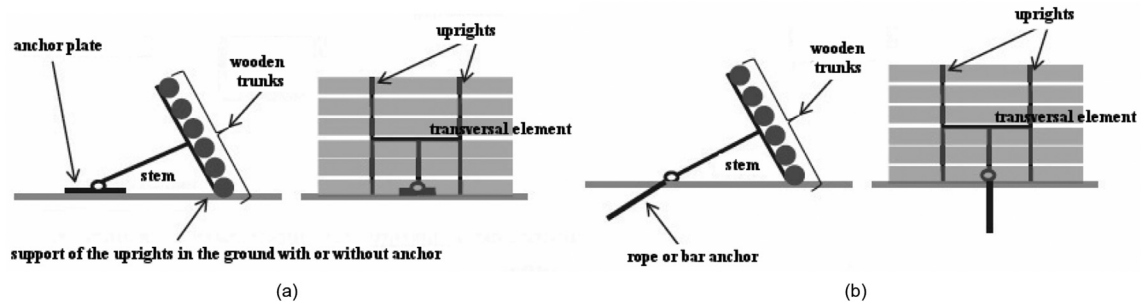


Fig. 3. Schematic drawing of a "TerraSafe" element with indication of its main components and both the foundation types: (a) plate and (b) anchorage.



Fig. 4. Example of the structure installed at Roatto (Asti, Italy): (a) the element before the filling, and (b) final configuration when the bushes start growing.





Fig. 5. (a) Filling phase and (b) placing of the upper alignments.

equal to  $\delta_a = 2\phi'/3 = 28^\circ$  because of the knurled steel surface of the base plate.

### 3. Experimental tests and results

The experimental test involved the installation of an alignment of three elements of the pIT. As stated previously, the central one was instrumented with:

- (1) Strain transducers (HBM SLB700A produced by HBM Messtechnik) in order to evaluate the state of stress at different sections (Fig. 7a) corresponding to the transducers from 1 to 8. Their properties are reported in Table 2.
- (2) Force and displacement transducers in order to evaluate the states of stress and strain at the foundation plate. The horizontal displacements of the foundation plate were measured using two displacement transducers (LVDT RDP DCW 1000B:  $\pm 25$  mm run), placed in front of the structure. Each transducer was placed in contact with the end of a steel bar, connected by a threaded ball joint to one side of the plate (Fig. 8). In order to assess the vertical forces acting on the anchor plate, four piezo-resistive transducers (Automation Projects AP400-6, capacity: 500 kg, precision: 1%) were placed at the four vertices of the foundation plate. A steel ribbed plate, placed above the transducers with the same size of the foundation plate and a central hole for the passage

of the stem, was used to distribute the vertical load onto the four measuring instruments (Fig. 9a).

- (3) A topographical survey in order to evaluate the displacements of the entire structure (Fig. 9b).

The upslope filling phase of the pIT was followed by the application of an overload made of eight cubic concrete blocks, each one having 1 m side length and 2400 kg mass (Fig. 7b). The eight concrete blocks are considered acting as a uniform load  $q$  equal to 32 kN/m<sup>2</sup>.

The topographic measurements on targets T1, T2, T3 and T4 showed that the displacements of the structure during the filling phase are generally vertical (Fig. 11). The uprights do not end with a base plate, so they sink into the ground and the sinking continues until the first bottom trunk reaches the ground, acting as a support for the structure. The downslope displacement of the structure is 70–90 mm for the lower targets and 130–150 mm with reference to the upper ones. These results show that, with increasing load, there is a small rotation of the structure induced by the soil filling.

The displacement measurement of the base plate has highlighted a downslope sliding of about 2 mm during the loading phase. These movements reached 10 mm with the application of the further overload (Fig. 12).

Fig. 9 and Table 3 give the location and the readings of force transducers located below the foundation plate. Transducer at location LT3 reached the full scale during the filling phase and then its last two readings cannot be interpreted. Transducer at location LT4 appeared to be at full scale from the beginning of the test, therefore it is supposed to be damaged. Remaining readings let to state that the soil above acts with the weight of a parallelepiped having base equal to that of the foundation plate and height equal to that of the filling sand.

Finally, the strain transducers on the steel frame allowed the evaluation of the internal forces (normal forces and bending moments) acting at selected sections (Fig. 13). When the structure is loaded, the strain transducers show a change in voltage corresponding to a certain strain. Knowledge of the elastic moduli makes possible to obtain the state of stress and so internal forces can be computed. The sections corresponding to the transducers from 1 to 6 are only subjected to bending moment, while at the attachment section of the stem with the horizontal beam, both bending moment and normal force act simultaneously.

The calculations were performed in the two final configurations of the test: when filling is completed (configuration I) and when overload is applied (configuration II). Tables 4 and 5 show the induced internal forces in the steel metal frame.



Fig. 6. View of the Fuscaldo (Cosenza) installation on the mountainside along a road. Elements of the structure were installed on two alignments one upon the other (Barbero et al., 2013).

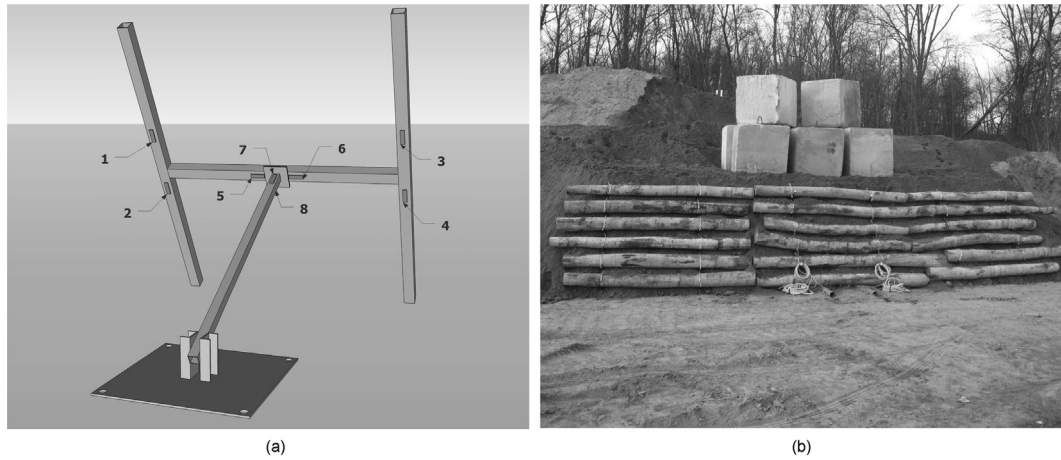


Fig. 7. (a) Locations of the strain transducers 1–8 installed, and (b) global view of the test site after overloading.



Fig. 8. View of the devices used for the measurement of the anchoring plate displacements.

Results show that, under the load presumably acting during lifetime (filling soil and possible overload), the stresses on the structure are compatible with the strength of steel frame and far from elastic limits. Following the reference frame as shown in Fig. 14a, the safety check, carried at the upper section of the anchor

beam after overload (Eq. (1)), confirms that the maximum stress  $\sigma_{\max}$  obtained by applying Navier formula is far from elastic limit  $f_{YK}$  of the steel frame:

$$\sigma_{\max} = \frac{N}{A} \pm \frac{M_X}{W_{el,X}} < f_{YK} \quad (1)$$

i.e.

$$58.57 \text{ MPa} = \frac{18900}{564} \text{ MPa} + \frac{209000}{8340} \text{ MPa} < 235 \text{ MPa}$$

where  $A$  is the area of the steel cross-section, and  $W_{el,X}$  is the elastic modulus along  $X$  axis of the upper section of the anchor beam. It should be noted that the study involved a configuration similar to that typical of serviceability conditions and it was not possible to analyze the ultimate strength of the pIT, due to the technical difficulty of applying such high loads.

The base plate must be adequately dimensioned in relation to the geotechnical properties of the foundation soil, in order to control the displacements. Taking into account the geological and geotechnical characteristics of the soil, it is also possible to increase the sliding strength by means of suitable fixing pegs. Additional measures could be also adopted to increase the roughness of the base plate and/or its size. Alternatively, same results can be

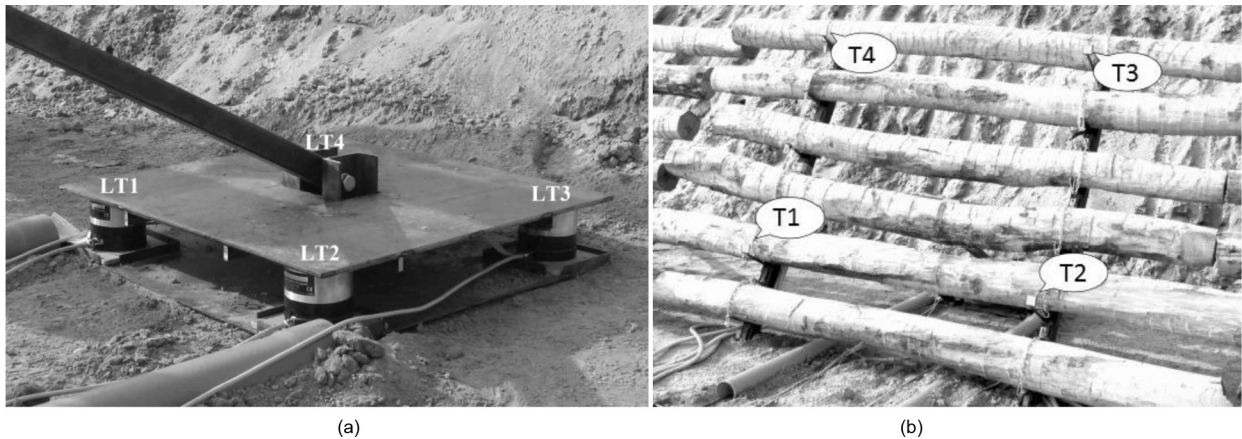


Fig. 9. (a) Load transducers (LT1, LT2, LT3, LT4) at the anchor plate, and (b) locations of the targets (T1, T2, T3, T4) for topographic measurements (modified from Barbero et al., 2013).

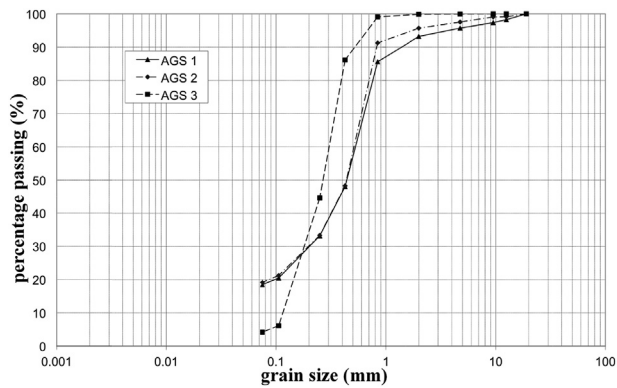


Fig. 10. Grain size distributions of three sandy samples used for the tests.

**Table 1**  
Geotechnical parameters of the filling sand.

Soil type	$\gamma$ (kN/m <sup>3</sup> )	$\varphi_{\text{peak}}$ (°)	$\varphi_{\text{critical state}}$ (°)	$c'$ (MPa)
Loose sand	12.5	42.6	37.1	0
Thickened sand	14.8	52.2	40.8	0

Note:  $\varphi_{\text{peak}}$  = peak friction angle;  $\varphi_{\text{critical state}}$  = friction angle at critical state;  $c'$  = cohesion.

obtained by fixing the end of the stem with an anchor rope or bar properly dimensioned and cemented into the ground.

4. Safety check procedure

The structure was developed to accept not negligible displacements and settlements during installation phase, therefore, the active thrust of the earth acting at the back of pIT is assumed to be

mobilized. It is necessary to divide the dimensioning procedure into two different analyses, as is frequently done for reinforced earth walls, gravity walls made with gabions, or other similar retaining structures (Lancellotta, 2009):

- (1) Internal stability (ultimate limit state) aimed at verifying the strength of the rod, the steel frame and the foundation anchor (with plate or rod);
- (2) External or global stability, which considers soil-cribwall as a gravity retaining wall. The earth thrust and any other possible overload are applied on it.

4.1. Internal stability

The internal stability analysis is aimed at checking against the sliding of the foundation (ultimate limit state) and the internal force capacity of the steel frame. The simplified two-dimensional geometry of the structure used for the static analysis is shown in Fig. 15 with all the symbols which will be used in the following procedure.

4.1.1. Reactions and sliding of the foundation

Assuming no water table, the actions to be considered are the active thrust of the soil ( $S_\gamma$ ) and the active thrust due to the overload on the top of the backfill ( $S_q$ ). The active thrust coefficient  $K_{a\gamma}$  and the thrust coefficient for the overload  $K_{aq}$  used in the calculations, proposed by Absi and Kerisel (1990), are listed in Table 6. The top of the backfill is assumed horizontal.

The active thrust of the soil mass is

$$S_\gamma = \frac{1}{2} K_{a\gamma} \gamma d (2b)^2 \tag{2}$$

**Table 2**  
Characteristics of the strain transducers.

Nominal strain (μm/m)	Nominal sensitivity (mV/V)	Maximum operative strain	Failure strain	Nominal displacement (mm)
500	1.5 ± 0.15	1.5	3	~ 0.038

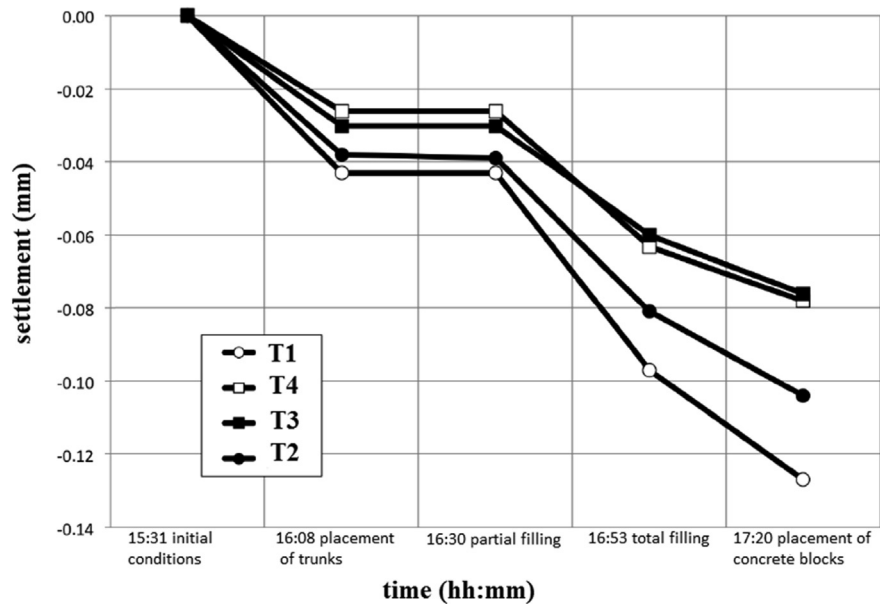


Fig. 11. Settlements obtained by topographic measurements on the targets T1, T2, T3 and T4.



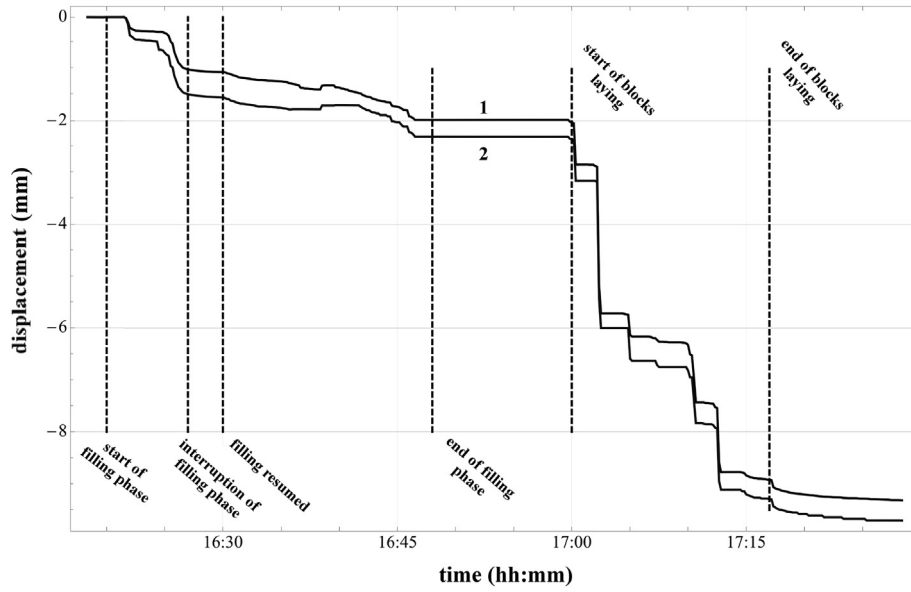


Fig. 12. Anchor plate displacements obtained by transducers 1 and 2 during the test.

This force is supposed to be applied to one-third of the height of the structure. The presence of a vertical overload  $q$  produces the thrust  $S_q$ :

$$S_q = K_{aq}q(2b) \quad (3)$$

This force is supposed to be applied at one-half of the height of the structure.

The unknown reaction components at the center of the plate and at the foot of the structure  $V$ ,  $H$  and  $F$  (Fig. 15) are obtained as solutions of the following equations:

(1) Horizontal equilibrium

$$H - (S_\gamma + S_q)\cos(\delta - \alpha) + F\sin\beta = 0 \quad (4)$$

(2) Vertical equilibrium

$$V - P + F\cos\beta - (S_\gamma + S_q)\sin(\delta - \alpha) = 0 \quad (5)$$

(3) Rotation around point O

$$\begin{aligned} -2Vb + P\frac{b}{2} + S_q\sin(\delta - \alpha)\frac{b}{2} + S_\gamma\sin(\delta - \alpha)\frac{b}{3} - S_q\cos(\delta - \alpha)\frac{h}{2} \\ - S_\gamma\cos(\delta - \alpha)\frac{h}{3} = 0 \end{aligned} \quad (6)$$

Solving simultaneously Eqs. (4)–(6),  $H$ ,  $F$  and  $V$  are obtained:

$$\begin{aligned} H = \frac{1}{12} \left[ 6\sqrt{3}(S_\gamma + S_q) \frac{\cos(\beta + \delta)}{\cos\beta} + 6(S_\gamma + S_q)\sin\delta \right. \\ \left. + (2S_\gamma\cos\delta - 9P)\tan\beta \right] \end{aligned} \quad (7)$$

$$V = \frac{P}{4} - \frac{1}{6}(2S_\gamma + 3S_q)\cos\delta \quad (8)$$

$$F = \frac{1}{12\cos\beta} [9P - 2S_\gamma\cos\delta + 6\sqrt{3}(S_\gamma + S_q)\sin\delta] \quad (9)$$

Knowledge of  $V$ ,  $H$  and  $F$  makes possible to check the sliding conditions of the foundation plate.

#### 4.1.2. Internal forces in the steel frame

The safety check of the steel frame is carried out in three different sections (Fig. 14a). The following internal forces acting at sections A, B and C are computed:

(1) Section C

$$N_C = H\cos\alpha - V\sin\alpha \quad (10)$$

$$T_{YC} = -(H\sin\alpha + V\cos\alpha), \quad T_{XC} = 0 \quad (11)$$

$$M_{XC} = \frac{3}{2}bV + \frac{1}{2}hH, \quad M_{YC} = 0, \quad M_{ZC} = 0 \quad (12)$$

(2) Section B

$$N_B = 0 \quad (13)$$

$$T_{YB} = \frac{-T_{YC}}{2}, \quad T_{XB} = \frac{N_C}{2} \quad (14)$$

$$M_{XB} = \frac{-T_{YCC}}{2}, \quad M_{YB} = \frac{-N_{CC}}{2}, \quad M_{ZB} = \frac{M_{XC}}{2} \quad (15)$$



(3) Section A

$$N_A + \frac{F}{2} - \frac{3}{8} S_\gamma \sin \delta - \frac{P}{4} \cos \alpha - \frac{S_q}{4} \sin \delta = 0 \quad (16)$$

$$T_{YA} - \frac{3}{8} S_\gamma \cos \delta + \frac{P}{4} \sin \alpha - \frac{S_q}{4} \cos \delta = 0 \quad (17)$$

$$M_{XA} - \frac{5h}{18} \frac{3}{8} S_\gamma \cos \delta + \frac{h}{4} \frac{P}{4} \sin \delta - \frac{h}{4} \frac{S_q}{4} \cos \delta = 0 \quad (18)$$

where  $N$  is the axial force;  $T_X$  and  $T_Y$  are the shear forces along  $X$  and  $Y$  axes, respectively;  $M_X$  and  $M_Y$  are the bending moments around  $X$  and  $Y$  axes, respectively; and  $M_Z$  is the torque around the longitudinal axis  $Z$  (Fig. 14b).

#### 4.2. External stability

In the external analysis, thrusts are applied on a virtual vertical plane located at the back of the anchor plate (Fig. 16). The loads transmitted to the pIT by the soil can be computed in a way similar to the usual retaining structures, considering the achievement of a condition of active thrust. Since the pIT allows drainage, calculations can be carried out in the absence of hydraulic thrust. If the soil used during the filling phase is considered not sufficiently permeable, it could be necessary to install a suitable drainage system behind and within the backfill, in order to minimize the water load. Assuming that this requirement is satisfied, Fig. 16 shows the following forces, per unit length, acting on the structure:

**Table 3**  
Readings of force transducers installed below the foundation plate.

Time (hh:mm)	Stage	Force (kN)			
		LT1	LT2	LT3	LT4
16:06	Initial reading	0	0	0	0
16:27	Filling phase (at half height)	1.59	1.47	2.95	0
16:48	End of filling phase	3.4	3.46	4.52	0
17:18	End of overloading phase	4.89	4.81	4.52	0

**Table 4**  
Computed bending moments  $M_X$  for the reference sections 1–6.

Configuration	$M_X$ (kN m)					
	Section 1	Section 2	Section 3	Section 4	Section 5	Section 6
I	0.169	0.169	0.777	0.338	0.118	0.203
II	0.253	0.203	1.081	0.405	0.203	0.253

**Table 5**  
Bending moments  $M_X$  and normal stresses  $N$  at the upper section of the anchor beam.

Configuration	$N$ (kN)	$M_X$ (kN m)
I	11.1	−0.176
II	18.9	−0.209

- (1) The active thrust  $S_\gamma$ , mobilized on the vertical plane at the back of the foundation plate;
- (2) The vertical force  $W$ , which is the sum of two components: the weight of the filling soil and the weight of the structure itself; and
- (3) The possible overload  $q$ , acting on the upper surface of the backfill, giving the thrust  $S_q$ .

The gradual filling phase on the backside was investigated experimentally in site test (Fig. 17). In this temporary situation, the safety of the structure can be verified, emphasizing the need for operators to act in order to prevent local instability phenomena. As it is frequently done for retaining structures (Lancellotta, 2009), also for the pIT, the external/global analysis should include the following items:

- (1) Check of the sliding conditions of the entire structure.
- (2) Bearing capacity check aimed at verifying the strength of the foundation soil.
- (3) Check of the toppling conditions. It is usually verified due to the squat sizes of the pIT.
- (4) Overall stability check. It is extremely meaningful if the pIT, suitable for shallow landslide stabilization, is placed in a slope.

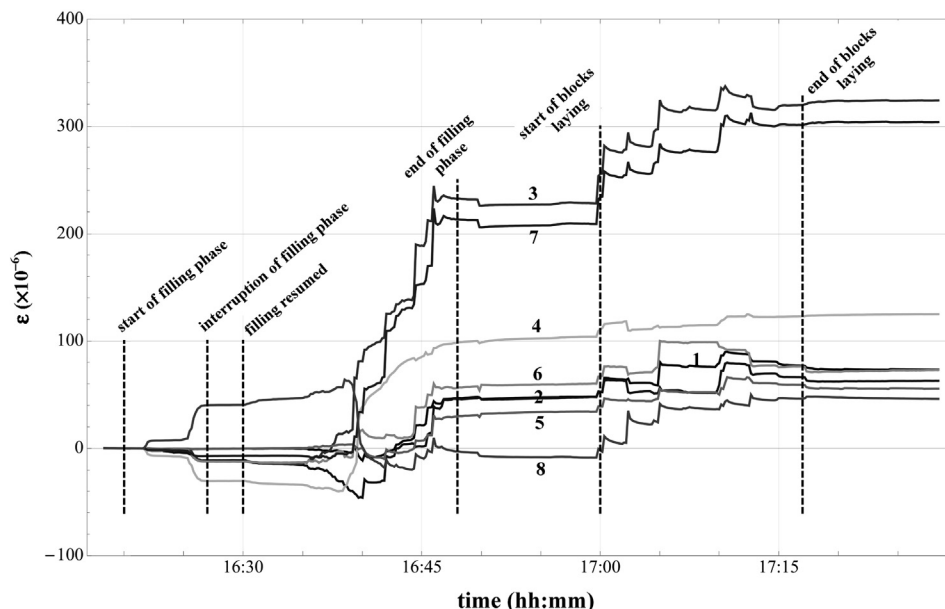


**Fig. 13.** Measured strains ( $\epsilon$ ) on the steel frame obtained by transducers 1–8 during the test.

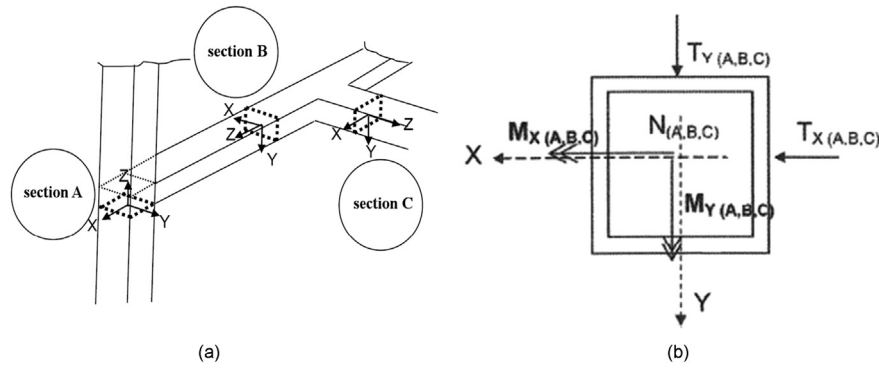


**Fig. 14.** (a) Reference system and position of the cross-sections used for the ultimate limit state check of the metallic frame, (b) internal forces and moments in the studied sections A, B and C.

## 5. Numerical example

A numerical analysis of the structure without overload is presented as an example of the design scheme previously described. The internal and external checks of the ultimate limit state of the structure can be performed according to the rules in force in each country. Among the different possibilities, the present example refers to Italian rules [NTC08 \(2008\)](#). According to [NTC08 \(2008\)](#), the input data ([Table 7](#)) are assumed as characteristic values of the real parameters obtained from laboratory tests. The given sizes correspond to the real dimensions of the tested prototype. The design values are then obtained by using the safety coefficients imposed by combination known as DA2 (Tables 6.2.I, 6.2.II and 6.5.I in [NTC08 \(2008\)](#)).

### 5.1. Internal stability: reactions

The characteristic value of the active thrust of the soil is

$$S_{\gamma,k} = \frac{1}{2} K_{\gamma} \gamma d (2b)^2 = 4.86 \text{ kN} \quad (19)$$

The design thrust of the soil  $S_{\gamma,d}$ , assumed as permanent non-structural unfavorable action, is obtained by considering the safety coefficient  $\gamma_{G2}$  (Table 6.2.I in [NTC08 \(2008\)](#)):

$$S_{\gamma,d} = S_{\gamma,k} \gamma_{G2} = 4.86 \times 1.3 = 6.3 \text{ kN} \quad (20)$$

Accordingly, using Eqs. (7)–(9), the design values of the reactions  $H_d$ ,  $V_d$  and  $F_d$  are obtained as 2.93 kN,  $-0.61$  kN and 6.59 kN, respectively.

### 5.2. Internal stability: sliding of the foundation

The foundation plate has two faces in contact with the soil (top and bottom) and it is also subjected to reaction's component  $V_d$ . The sliding strength  $R_d$  is calculated as

$$R_d = (2W_s - V_d) \tan \delta_a \quad (21)$$

where  $W_s$  is the weight of the soil acting above the foundation plate, in accordance to the recorded data by the load transducers at the anchor plate ([Fig. 9a](#)):

$$W_s = \gamma h A_{\text{plate}} = 15 \times 1.8 \times 0.75 \times 0.75 = 15.2 \text{ kN} \quad (22)$$

Therefore, the internal sliding strength can be calculated according to Eq. (21):  $R_d = (2 \times 15.2 + 0.6) \tan 28^\circ = 16.5 \text{ kN}$ .

Safety against the ultimate limit state of sliding requires the following inequality:

$$H_d < \frac{R_d}{\gamma_R} \quad (23)$$

Knowledge of the safety coefficient  $\gamma_R$  from the Italian rules (Table 6.5.I in [NTC08 \(2008\)](#)) shows that the check is therefore satisfied by the example data, because  $2.9 \text{ kN} < 16.5/1.1 \text{ kN} = 15 \text{ kN}$ .

### 5.3. Internal stability: structural check of the steel frame

In order to perform the internal structural check,  $c = 0.785 \text{ m}$  is defined as the half-distance between the uprights. Geometric input data of steel sections (area  $A$  and strength module  $W$ ) are given: (1) For section C:  $A_C = 0.000564 \text{ m}^2$ ,  $W_C = 8.34 \times 10^{-6} \text{ m}^3$ ; (2) For sections A and B:  $A_A = A_B = 0.000804 \text{ m}^2$ ,  $W_A = W_B = 17.2 \times 10^{-6} \text{ m}^3$ .

With reference to the design approach previously proposed, internal forces  $\sigma_i$  in sections A, B and C computed using Eqs. (10)–(18) are summarized in [Table 8](#). In each section, knowledge of the safety coefficient  $\gamma_M$  from the Italian rules (Table 4.2.V in [NTC08 \(2008\)](#)) makes the check satisfied if the following inequality is met:

$$\sigma_i < \frac{f_{yk}}{\gamma_M} = \frac{235}{1.05} = 224 \text{ MPa} \quad (24)$$

In this case, all sections are verified:

#### (1) Section A

$$\sigma_i = \frac{N}{A} + \frac{M_X}{W_X} - \frac{M_Y}{W_Y} = \frac{-0.91}{8.04 \times 10^{-4}} + \frac{0.68}{17.2 \times 10^{-6}} - \frac{0}{17.2 \times 10^{-6}} = 38.4 \text{ MPa} < 224 \text{ MPa} \quad (25)$$

#### (2) Section B

$$\sigma_i = \frac{N}{A} + \frac{M_X}{W_X} - \frac{M_Y}{W_Y} = \frac{0}{8.04 \times 10^{-4}} + \frac{-0.37}{17.2 \times 10^{-6}} - \frac{-1.11}{17.2 \times 10^{-6}} = 43 \text{ MPa} < 224 \text{ MPa} \quad (26)$$



**Table 7**

An example of application of the design scheme: Characteristic values of input data.

$\beta$ (°)	$\phi'$ (°)	$P$ (kN)	$\delta_a$ (°)	$\gamma$ (kN/m <sup>3</sup> )	$l$ (m)	$h$ (m)	$q$ (kPa)	$d$ (m)	$c$ (m)	$K_{a\gamma}$	$K_{aq}$	$f_{yk}$ (MPa)	$S_q$ (kN)
30	40	4	28	15	0.75	1.8	0	3	0.785	0.05	0.09	235	0

**Table 8**Values of internal forces ( $T_X$ ,  $T_Y$ ,  $N$ ), bending moments ( $M_X$ ,  $M_Y$ ,  $M_Z$ ) and maximum stresses (Max.  $\sigma_x$ , Max.  $\tau$ ) computed for the structural design in sections A, B and C.

Section	$T_X$ (kN)	$T_Y$ (kN)	$N$ (kN)	$M_X$ (kN m)	$M_Y$ (kN m)	$M_Z$ (kN m)	Max. $\sigma_x$ (MPa)	Max. $\tau$ (MPa)	$\sigma_i$ (MPa)
A	0	1.31	−0.91	0.68	0	0	41	~0	41
B	1.42	0.47	0	−0.37	−1.11	0.84	86	1	86
C	0	−0.93	2.84	1.68	0	0	206	5.4	206

As in the previous case,  $\gamma_R = 1.1$  lets to assume that the check is satisfied by the example data, because  $9.2 > 1.1$ .

## 6. Numerical model

With reference to the strain measurements recorded by gage transducers placed on the metallic frame, a numerical simulation of the structure was carried out. A finite element code Dolmen was used for modeling the pIT in the configuration in which it is loaded by the upslope overload consisting of eight concrete blocks. The numerical model was successfully validated by applying on the top of the oblique uprights two concentrated forces  $F$  (1000 N each one) perpendicular to the uprights. Elastic materials properties are summarized in Table 9.

Defining  $m$  as the mass of each of the  $n$  blocks placed in order to have a total footprint equal to  $A = 6 \text{ m}^2$ , the overload  $q$  was calculated and applied to the structure as an uniform load:

$$q = \frac{mn}{A} = \frac{2400 \times 8}{6} = 32 \text{ kPa} \quad (34)$$

The presence of the vertical overload  $q$  produces a thrust  $S_q$ :

$$S_q = K_{aq}q(2b) = K_{aq}q(2htan\alpha) = 5.08 \text{ kN} \quad (35)$$

Considering the influence width  $L_i$  of each trunk, the thrust  $S_{q,i}$  of each trunk is obtained:

$$S_{q,i} = S_q L_i \quad (36)$$

This thrust is considered in the numerical model as permanent load. Then, in the same location of the instrumented points, normal force ( $N$ ) and bending moments ( $M_Y$ ,  $M_Z$ ) are obtained. Stresses ( $\sigma$ ) due to the overload were then calculated by using Navier formula, in order to evaluate the corresponding strains ( $\epsilon$ ):

$$\epsilon = \frac{\sigma}{E} = \frac{\frac{N}{A} + \frac{M_Y}{W_Y} - \frac{M_Z}{W_Z}}{E} \quad (37)$$

Such strains  $\epsilon$  are compared with strains  $\epsilon^*$  recorded by gage transducers located at the same positions (Fig. 7a). These strains  $\epsilon^*$  were obtained as the difference between the strains  $\epsilon'(I)$  and  $\epsilon'(II)$  due to the thrust of the filling soil under configurations I and II, as shown in Table 10. Before comparing  $\epsilon$  and  $\epsilon^*$ , the measured strains  $\epsilon'$  were appropriately adjusted in order to consider the influence of the thickness ( $t$ ) and the width ( $w$ ) of the plate on which the measurement takes place (Fig. 18):

$$\epsilon^* = [\epsilon'(II) - \epsilon'(I)]\lambda(t, w) \quad (38)$$

**Table 9**

Material properties of the TerraSafe structure.

Material	$E$ (MPa)	$\nu$	$G$ (MPa)	$\alpha^*$ (°C <sup>−1</sup> )
Steel	$2.1 \times 10^5$	0.3	$8.1 \times 10^4$	$1 \times 10^{-5}$
Wood	$1 \times 10^4$	0.25	$6 \times 10^3$	0

Note:  $E$  = elastic modulus;  $\nu$  = Poisson's ratio;  $G$  = shear modulus;  $\alpha^*$  = thermal coefficient.

**Table 10**Recorded values of the strains in the reference configurations, multiplied by  $10^{-6}$ .

Configuration	$\epsilon'_1$	$\epsilon'_2$	$\epsilon'_3$	$\epsilon'_4$	$\epsilon'_5$	$\epsilon'_6$	$\epsilon'_7$	$\epsilon'_8$
I	50	50	230	100	35	60	210	−10
II	75	60	320	120	60	75	300	40

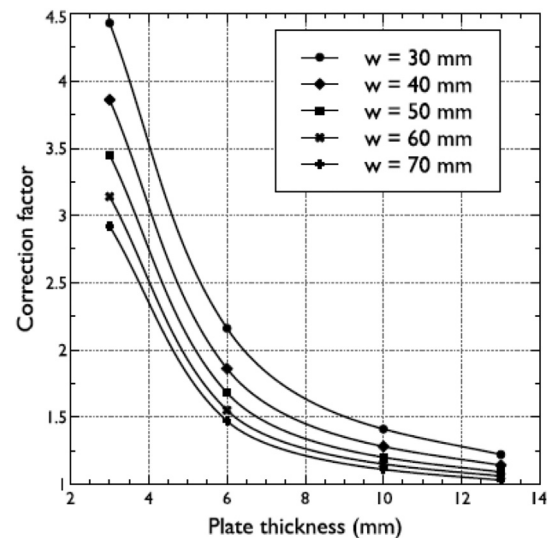


**Fig. 18.** Relationships between correction factor ( $\lambda$ ) and thickness ( $t$ ) of the plate for different values of width  $w$  (Borri-Brunetto et al., 2016).



**Table 11**

Recorded values of the strains multiplied by  $10^{-5}$  and corrected basing on the thickness of the plate and the width of the side on which the measurement takes place.

$\varepsilon_1^*$	$\varepsilon_2^*$	$\varepsilon_3^*$	$\varepsilon_4^*$	$\varepsilon_5^*$	$\varepsilon_6^*$	$\varepsilon_7^*$	$\varepsilon_8^*$
7.13	2.85	0.257	5.7	7.13	4.28	0.311	0.104

**Table 12**

Computed values of the strains multiplied by  $10^{-4}$  obtained from finite element analysis.

$\varepsilon_1$	$\varepsilon_2$	$\varepsilon_3$	$\varepsilon_4$	$\varepsilon_5$	$\varepsilon_6$	$\varepsilon_7$	$\varepsilon_8$
8.894	6.44	8.3	6.31	34.3	33.7	2.95	2.95

Strains  $\varepsilon'(I)$  and  $\varepsilon'(II)$  are the recorded values for configurations I and II, while  $\lambda$  is the correction factor related to the thickness (3 mm) and the width (70 mm and 50 mm for strain transducers 1–6 and 7 and 8, respectively) of the plate. The modeling was then repeated by changing the boundary conditions, according to three different constraints applied at the base of the steel uprights:

- (1) Spherical hinge. As external constraint, a spherical hinge was chosen and placed at the base of the uprights, thus allowing their rotation.
- (2) Inclined roller. As external constraint, an inclined roller was chosen. It has the same angle of the face of the pIT.
- (3) Vertical roller. As external constraint, a vertical roller was chosen and placed at the base of the uprights, thus allowing the horizontal shifting along X direction, following the reference system OXYZ, as shown in Fig. 14a.

Strains measured on the structure ( $\varepsilon^*$ ) are listed in Table 11. They are one or two orders of magnitude lower than strains ( $\varepsilon$ ) calculated within the Caquot-Kerisel theory, as shown in Table 12. Finally, numerical modeling shows that the strains and stresses obtained at locations 1–8 seem not to change significantly by applying different constraints at the base of the steel uprights.

## 7. Conclusions

An in situ campaign, described in Section 2, allowed to study the stress-strain behavior of an innovative prefabricated structure, pIT, for shallow landslide stabilization. The pIT consists of a metal frame completely immersed in the soil and a face made of tree trunks acting as containment for the unstable wedge, among which scions or autochthonous bushes are planted. As shown in Section 3, the use of a metal frame allows to obtain good performance, in terms of strength and rate of assembly. Indeed, the pIT is a prefabricated structure, economical and easy to assemble or transport. It does not need any concrete foundation, but only an anchor plate, a rope or a bar anchor cemented into the ground. Because of its steel frame, the pIT has a higher structural resistance and durability if compared to other bio-engineering structures made entirely of wood, such as Roma or Vesuvio double cribwalls. Furthermore, the pIT is currently adopted as an environmental sustainable solution for several landslide stabilization (Roatto and Fuscaldo, Italy), by creating multiple alignment lines of each modular element.

A simple design method, shown in Section 4 and applied in Section 5, was proposed for the structural and geotechnical design of pIT. Despite the introduction of some simplifications about

geometry and behavior of the structure, as shown in Section 5, the pIT was verified from the structural and geotechnical point of view, letting to assume the proposed approach is reliable and realistic.

Numerical modeling with a finite element code, described in Section 6, allowed to understand that the overload applied on the structure was not equal to that required for the mobilization of the active thrust and for the creation of the failure wedge at upslope of the pIT. Strains measured on the structure are significantly lower, one or two orders of magnitude, than those calculated within the ultimate limit state by Caquot-Kerisel theory. Moreover, it has to be highlighted that the numerical models represent an ideal situation of symmetry of loading and strain. Indeed, the measured strain values are affected by the history of the operations performed on site, such as the non-simultaneous positioning of the overload.

Finally, the presented design method must be adapted to the conditions of the site, taking into account the site-specific geotechnical parameters and boundary conditions, and considering the overall procedure as a useful reference guideline.

## Conflict of interest

We wish to confirm that there are no known conflicts of interest associated with this publication and there has been no significant financial support for this work that could have influenced its outcome.

## Acknowledgements

The authors wish to thank A. Valfrè for his helpful suggestions for the realization of this work and P. Fea of P.M.P. Costruzioni Srl, who realized the structures. This work was developed in the research contract No. 421/2012: “Studi inerenti opere innovative per la stabilizzazione di pendii in terra” between PMP Costruzioni S.r.l. and DIATI Politecnico di Torino.

## References

- Abis E, Kerisel J. Active and passive earth pressure tables. Taylor and Francis Group; 1990.
- Barbero M, Barpi F, Borri-Brunetto M, Pallara O, Peila D, Peila L, Valfrè A, Cornolini P. Comportamento di una palificata prefabbricata per il contenimento delle terre: studi sperimentali. *Geotecnica Ambientale e Mineraria* 2013;138(1):5–12 (in Italian).
- Barbero M, Barpi F, Borri-Brunetto M, Peila D. Principi di dimensionamento della palificata loricata Terrasafe. *Geotecnica Ambientale e Mineraria* 2014;142(3):43–8 (in Italian).
- Borri-Brunetto M, Alessio M, Barbero M, Barpi F, De Biagi V, Pallara O. Stiffening effect of bolt-on transducers on strain measurement. *Latin American Journal of Solid and Structures* 2016;13:536–53.
- Campbell SDG, Shaw R, Sewell RJ, Wong JCF. Guidelines for soil bioengineering applications on natural terrain landslide scars. GEO special project report. Hong Kong, China: Geotechnical Engineering Office, Civil Engineering Department, the Government of Hong Kong Special Administrative Region; 2006.
- Carbonari A, Mezzanotte M. Tecniche naturalistiche nella sistemazione del territorio. Provincia Autonoma di Trento 2000 (in Italian).
- Cornolini P, Sauli G. Manuale di indirizzo delle scelte progettuali per interventi di ingegneria naturalistica – Ministero dell'Ambiente e della Tutela del Territorio, Ministero dell'Economia e delle Finanze. In: *Operative project land defence*. Roma: Poligrafico e Zecca dello Stato; 2005. p. 350–4 (in Italian).
- Cornolini P, Sauli G. Principi, metodi e deontologia dell'ingegneria naturalistica. Regione Lazio; 2012 (in Italian).
- Cornolini P. La palificata viva Roma: una nuova tipologia di ingegneria naturalistica. *Acer* 2001;1:70–1 (in Italian).
- De Antonis L, Molinari VM. Interventi di sistemazione del territorio con tecniche di ingegneria naturalistica. Regione Piemonte; 2003 (in Italian).
- EN 1997-1. Eurocode 7: geotechnical design – Part 1: general rules. European Committee for Standardization; 2004.
- Gray DH, Sotir RB. Biotechnical and soil bioengineering slope stabilisation: a practical guide for erosion control. New York: Wiley; 1996.
- Greenway DR. Vegetation and slope stability. New York: John Wiley and Sons; 1987.
- Lancellotta R. Geotechnical engineering. Taylor and Francis; 2009.

- Morgan RPC, Rickson RJ. Slope stabilization and erosion control: a bioengineering approach. London: Taylor and Francis; 2004.
- Norris JE, Stokes A, Mickovski SB, Cammeraat E, van Beek R, Nicoll BC, Achim A. Slope stability and erosion control: ecotechnological solutions. Springer; 2008.
- NTC08. Italian building codes: DM Infrastrutture 14 gennaio 2008. Rome: Department of Civil Protection; 2008 (in Italian).
- Provincia di Terni. Manuale Tecnico di Ingegneria Naturalistica della Provincia di Terni: Applicabilità delle tecniche, limiti e soluzioni. Servizio Assetto del Territorio – Ufficio Urbanistica; 2003 (in Italian).
- Stokes A, Douglas GB, Fourcaud T, Giadrossich F, Gillies C, Hubble T, Kim JH, Loades KW, Mao Z, McIvor IR, Mickovski SB, Mitchell S, Osman N, Phillips C, Poesen J, Polster D, Preti F, Raymond P, Rey F, Schwarz M, Walker LR. Ecological mitigation of hillslope instability: ten key issues facing researchers and practitioners. *Plant and Soil* 2014;377(1):1–23.
- Stokes A, Mickovski SB, Thomas BR. Eco-engineering for the long-term protection of unstable slopes in Europe: developing management strategies for use in legislation. In: Lacerda W, Ehrlich M, Fontoura SAB, Sayao ASF, editors. IX international society of landslides conference. A.A. Balkema; 2004. p. 1685–90.
- Stokes A, Sotir R, Chen W, Ghestem M. Soil bio- and eco-engineering in China: past experience and future priorities. *Ecological Engineering* 2010;36(3):247–57.
- Stokes A, Spanos I, Norris JE, Cammeraat E. Eco and ground bio-engineering: the use of vegetation to improve slope stability. In: Proceedings of the 1st international conference on eco-engineering. Springer; 2007. p. 165–73.
- United States Department of Agriculture (USDA), Natural Resources Conservation Service (NRCS). Soil bioengineering for upland slope protection and erosion reduction. In: Chapter 18 of engineering field handbook. Washington, D.C.: USDA; 1992.

Victor E, Bary C. Mechanically stabilized earth walls and reinforced soil slopes. Washington, D.C.: U.S. Department of Transportation; 1997.



**Gianluca Bella** is currently a PhD candidate in Environmental Engineering at Department of Structural Building and Geotechnical Engineering of Politecnico di Torino. In 2013, he obtained a MS degree in Geotechnical Engineering from the same University. He worked as geotechnical and structural engineer in a private company since 2013. During his doctorate, in 2016, he spent 3 months at Centro de Desenvolvimento da Tecnologia Nuclear (CDTN) and Universidade Federal de Minas Gerais (UFMG) in Belo Horizonte (Brasil), improving his knowledge on experimental investigation of tailing materials. His main research includes the study of soils in unsaturated conditions, especially regarding the geotechnical characterization of tailing wastes. He is now focussing on the mechanical and hydraulic behavior of unsaturated soils with special regard to the possible onset of static liquefaction and occurrence of critical state. His research interests also cover physical and chemical characterization of aged tailings. With his research group, he proposed an innovative accelerated aging technique to simulate the natural ionizing radiation of tailings. He attended, as author, several national and international conferences focused on soil mechanics and rock mechanics.